International Journal of Fatigue 95 (2017) 38–44

Contents lists available at ScienceDirect

International Journal of Fatigue

journal homepage: www.elsevier.com/locate/ijfatigue

Generalized evaluation method for determining transition crack length for microstructurally small to microstructurally large fatigue crack growth: Experimental definition, facilitation, and validation

Toshinobu Omura, Motomichi Koyama *, Yasuaki Hamano, Kaneaki Tsuzaki, Hiroshi Noguchi

Department of Mechanical Engineering, Kyushu University, Motooka 744, Fukuoka, Fukuoka 819-0395, Japan

ARTICLE INFO

Article history:
Received 25 July 2016
Received in revised form 27 September 2016
Accepted 6 October 2016
Available online 6 October 2016

Keywords:
Fatigue crack growth
Microstructurally small crack
Probabilistic analysis
Focused ion beam

ABSTRACT

We proposed a generalized method to determine the transition crack length from a microstructurally small to a microstructurally large crack growth, l_0. Artificial errors are minimized in the data analysis process of the proposed method. In this study, we used low carbon steel specimens, each with eight micro notches (the ferrite grain size was 25 μm). The micro notches were introduced by focused ion beam technique, which is regarded as pre-cracks in steel. The obtained l_0 (188 μm) agrees with previous studies. With the present specimen geometry, l_0 can be determined using two specimens—an approach that is much easier than conventional methods.

1. Introduction

In order to increase energy efficiency, structural parts must have high strength. As the total volume of parts in any structure can be reduced by strengthening the materials themselves, the total weight of a structure, such as an automobile, can be decreased accordingly. The most important strength parameter is fatigue strength and the associated fatigue life. However, fatigue strength and life are known to be scattered [1,2]; the degree of scatter is a crucial consideration to determine the safety factor. A structural material with a high safety factor cannot be effectively utilized even if it has a superior high fatigue strength. Accordingly, for material design and selection to reduce weight, we have to consider two factors: fatigue strength and the degree of scatter in both fatigue strength and life. The former parameter has been measured with well-defined methods, e.g., rotating bending fatigue testing, bending fatigue testing, and uniaxial tension-compression fatigue testing, etc., whereas the scatter in fatigue strength and fatigue life still need further study in order to achieve a more quantitative and an advanced structure design.

The most important phenomenon related to the scatter is recognized to be small fatigue crack growth [3]. Small fatigue crack growth in many structure materials dominates a major part of fatigue life [4,5]. In fact, the fatigue crack growth rate is probabilistic depending on the microstructure characteristics at a crack tip [6–8]. Therefore, the small crack defined by the probabilistic fatigue crack growth behavior is called as microstructurally small crack [3,9]. The growth behavior of the microstructurally small crack is a primary factor causing the scatter in the many structure materials. More specifically, Goto [1] reported that the scattering of crack growth rate disappeared when the crack length grew over a few hundred μm in low carbon steels. In their paper, the transition crack length from a microstructurally small to a microstructurally large fatigue crack growth was defined as l_0 and is considered to be an indispensable parameter in understanding scatter in fatigue life. This evaluation method of l_0, however, requires a considerable number of fatigue crack propagation experiments for statistical analysis [1,10] rendering this approach too difficult to be considered a universal evaluation methodology.

In this paper, we demonstrate our efforts in addressing two challenges in sophisticating the evaluation of l_0. First, a facilitated experimental method to determine l_0 is proposed. Then, we discuss how the experimentally defined l_0 can be applied as a reliable parameter in predicting fatigue. This paper documents basic research to establish a mechanical and probabilistic evaluation/prediction method for fatigue life of structure bodies.

* Corresponding author.
E-mail address: koyama.motomichi.406@m.kyushu-u.ac.jp (M. Koyama).

http://dx.doi.org/10.1016/j.ijfatigue.2016.10.010
0142-1123/

2. Experimental procedure

2.1. Material and specimen geometry

A commercial low carbon steel (JIS S10C) was used in this study. The chemical composition and the mechanical property of the steel are documented in Tables 1 and 2. The steel was annealed at 1173 K for 1 h and then furnace-cooled to room temperature. The initial structure consists of ferrite with a small amount of pearlite. The ferrite grain size was approximately 25 μm.

The fatigue crack growth behavior was evaluated by Ono-type rotary bending fatigue testing. Fig. 1a shows the specimen geometry. The fatigue specimens were prepared by lathe. The specimens were first ground by #280-#2000 emery papers polished by a buff with 1 μm alumina particles and then etched with 3% Nital. Eight micro-notches were then introduced by focused ion beam (FIB) for the subsequent experiment. The FIB notches were introduced at 30 kV and 15 nA. A schematic illustration and an actual image of the FIB notch are shown in Fig. 1b and c. The FIB notch geometry has been reported to be regarded as a sharp pre-crack in fatigue testing [11]. Fatigue crack length was measured as total projected surface crack length including the FIB notch as schematically shown in Fig. 2. In order to statistically analyze the probabilistic properties of small fatigue crack growth behavior, three specimens containing eight FIB notches were tested. In this paper, the three specimens are referred to as No. 1, No. 2, and No. 3, respectively. To avoid elastic interactions between cracks, an interval of each FIB notch was set to be 2 mm based on Saint-Vanent's principle.

2.2. Fatigue test and evaluation method of l_0

The fatigue testing was carried out at 60 Hz in air at room temperature. The stress amplitude and stress ratio were selected to be 250 MPa, and $R = -1$. In this experiment, the nominal stress was defined as the nominal bending stress in the minimum diameter zone without considering the effects of the stress concentration source shape. Observations of the fatigue crack growth behavior and measurements of the fatigue crack length were carried out through the replica technique. Replication was conducted after immersing an acetyl cellulose replica film into methyl acetate under a no-load condition. Replica images were taken by optical microscopy after spattering Au on the replica surface.

3. Experimental result

Fig. 2 shows the fatigue crack length plotted against the number of cycles for the three specimens containing eight FIB notches each. Fig. 3 shows corresponding fatigue crack growth rates plotted against number of cycles. As seen in Fig. 3, the fatigue crack growth rates show various values even at a given crack length particularly when the cracks are small. Table 3 shows the corresponding fatigue crack lengths for each crack at 1.9×10^5 cycles where the fatigue test nearly reaches the final stage. In this study, we analyzed the scatter of the fatigue crack growth behavior by using this crack growth data.

Note that the fatigue crack growth behavior sometimes shows scatter even for longer fatigue crack lengths as seen in Fig. 3. In other words, the scatter of fatigue crack growth rates does not disappear (crack growth rate curves sometimes show irregular behavior), which complicates the analysis of the threshold crack length of microstructurally small crack growth regime, l_0. Thus, we need to have a solution to determine the reproducible and quantitative l_0. A methodology is presented in the following section.

Table 2
Mechanical property of the low carbon steel (JIS S10C).

Yield strength	Tensile strength	Total elongation
220 MPa	350 MPa	33%

4. Analysis and discussion

4.1. Experimental definition of l_0

In contrast to the local crack growth rate, the global fatigue crack growth rate corresponding to the fatigue life is relatively stable. Here, the local crack growth rate means values obtained from a difference between respective data, which is conventional fatigue crack growth rates shown in Fig. 3. The global fatigue crack growth rate means values obtained by dividing total fatigue crack length by total number of cycles. Fig. 4 shows an example of the relationship between the fatigue crack length and the number of cycles, which demonstrates global fatigue crack growth behaviors of the longest cracks in each specimens. The linear relationship between logarithmic crack length and number of cycles presented in Fig. 4 is typical behavior of a crack that does not satisfy the small scale yielding condition [12,13]. The average value of slopes of the linear relationship in a range until a crack length of 1 mm obtained from all cracks of the three specimens was measured to be 16.9×10^{-3} with a standard deviation of 1.41×10^{-3}.

Here, as shown in Fig. 5, global fatigue crack growth rate is defined as

$$\left(\frac{dl}{dN}\right)_g = \frac{l - 50\ \mu\text{m}}{N} \tag{1}$$

where l is the crack length (μm), N is the number of cycles, and 50 μm is the length of the FIB notch. As the global fatigue crack growth rate for a long crack length is stable, the standard deviation of the global fatigue crack growth rate decreases with the crack length.

The calculated global fatigue crack growth rate against crack length for cracks longer than 1 mm is shown in Fig. 6. According to Saint-Vanent's principle, the cracks did not elastically interact with each other when they were small. As seen in Fig. 6, scatter of global fatigue crack growth rates converges gradually when the global fatigue crack is logarithmically plotted against crack length. The distinct scatter in global fatigue crack growth rate can be correlated with not only local resistance to plastic straining at a crack tip but also a difference in crack growth mechanisms between small and large cracks. In an early fatigue crack growth, the fatigue crack propagates along slip planes because of localized dislocation accumulation [14] and partly propagates through alternating operation of slip planes [15]. Then, increasing crack length changes the predominant fatigue crack growth mechanism to crack blunting and re-sharpening type [16,17]. The early fatigue crack growth behavior is sensitive against active slip systems [15,18]

Table 1
Chemical composition of the low carbon steel in wt.% (JIS S10C).

C	Si	Mn	P	S	Cu	Al	Ni + Cr	Fe
0.13	0.22	0.39	0.01	0.02	0.09	0.01	0.01	Bal.

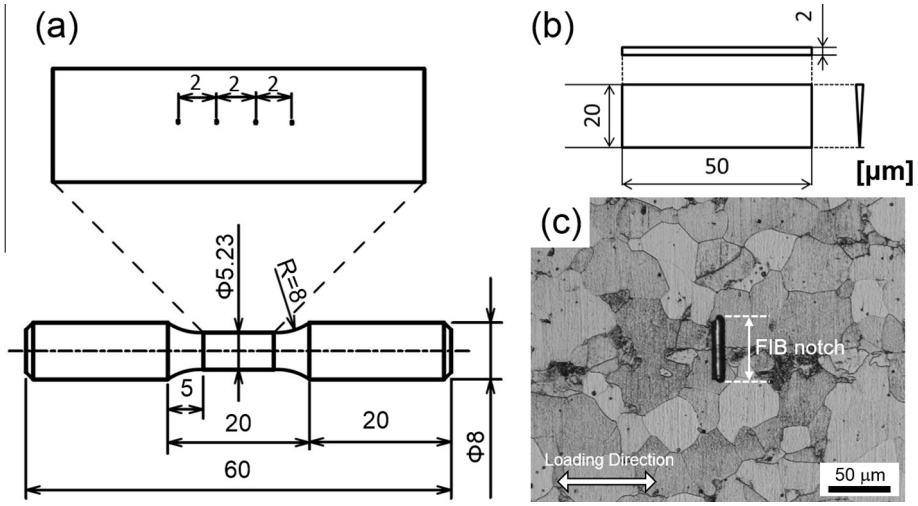

Fig. 1. (a) Shape of a fatigue specimen with FIB notches. The schematic illustration of the specimen shows four FIB notches with an interval of 2 mm. The rest four notches were introduced on the backside of the specimen. (b) Geometry of the FIB notch. (c) Optical micrograph of the initial microstructure, including the FIB notch.

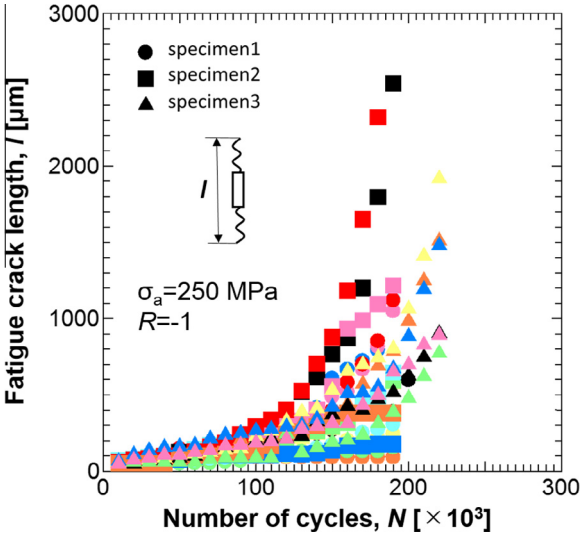

Fig. 2. Fatigue crack length plotted against number of cycles.

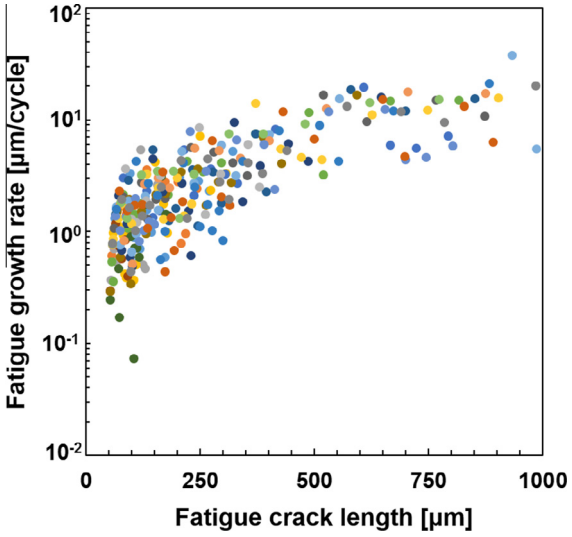

Fig. 3. Fatigue crack growth rate plotted against fatigue crack length.

and presence of barriers to dislocation motion such as grain boundaries [19–21] at a crack tip, whereas crack growth rates associated with blunting and re-sharpening mechanism reach a specific mean value with evolution of a plastic zone size at a crack tip. Accordingly, the logarithmic global fatigue crack growth rates also showed the large scatter in the early fatigue stage, and converged later. From the data in Fig. 6, the standard deviation of the logarithmic global fatigue crack growth rate was obtained as shown in Fig. 7. Standard deviation of the logarithmic fatigue crack growth rate was calculated by

$$\sigma = \sqrt{\frac{\sum_{i=1}^{n}(x_i - \bar{x})^2}{n}} \tag{2}$$

where x and $\bar{x}$ are logarithmic global fatigue crack growth rate and that of mean, and n is number of global fatigue crack growth rate data used for the calculation. Although the logarithmic global fatigue crack growth rate is dimensionless, calculation of the values is based on a unit of μm/cycle. In order to obtain continuous curves of the standard deviation, logarithmic global fatigue crack growth rates for respective crack lengths were estimated by linear interpolation between the nearest two experimental data points.

As the definition of l_0 is a transition crack length from scattered to less-scattered propagation behavior, the standard deviation of the logarithmic global fatigue crack growth rate decreases with the crack length. The standard deviation of the logarithmic global fatigue crack growth rate reaches the standard deviation of the final logarithmic global fatigue crack growth rate. Namely, when the slope in the relation between the standard deviation of the logarithmic global fatigue crack growth rate and the crack length is drastically changed, the corresponding crack length is determined to be l_0. Note that the change in standard deviation in Fig. 7 is gradual, although the change in slope is drastic as we expected. A tangent method to determine the quantitative l_0 is not available, as the curve shape is more or less wavy around the presumable position of l_0. Instead, two approximation lines were drawn by least squares method for microstructurally small and long crack regions. The detailed procedure for determination of optimal approximation lines consists of three steps as explained below.

1. Set an arbitrary point (X, Y) as shown in Fig. 7.
2. Define two linear approximate equations described as Eqs. (3) and (4), which satisfy Eqs. (5) and (6).

Table 3
Length of fatigue cracks at 1.9×10^4 cycles that initiated from the respective FIB notches. Crack length of 50 μm indicates no crack initiation from the FIB notch.

Specimen number	1							
FIB notch number	1	2	3	4	5	6	7	8
Fatigue crack length (μm)	389	242	156	306	1121	1048	1119	90
Specimen number	2							
FIB notch number	1	2	3	4	5	6	7	8
Fatigue crack length (μm)	2542	50	593	646	175	1216	3424	379
Specimen number	3							
FIB notch number	1	2	3	4	5	6	7	8
Fatigue crack length (μm)	515	803	387	50	673	650	50	785

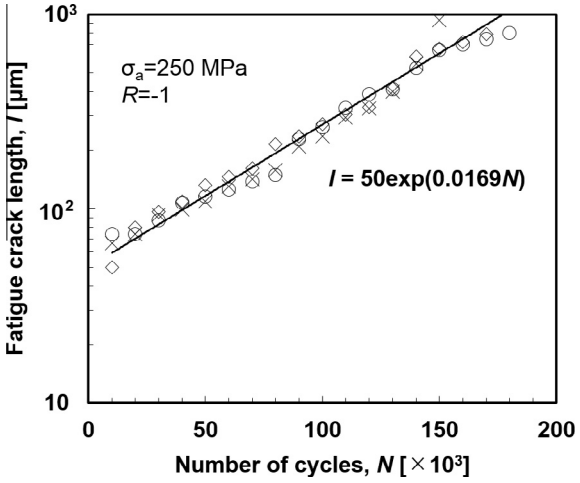

Fig. 4. An example of the relationship between fatigue crack length and number of cycles. Three typical data sets were selected in this diagram.

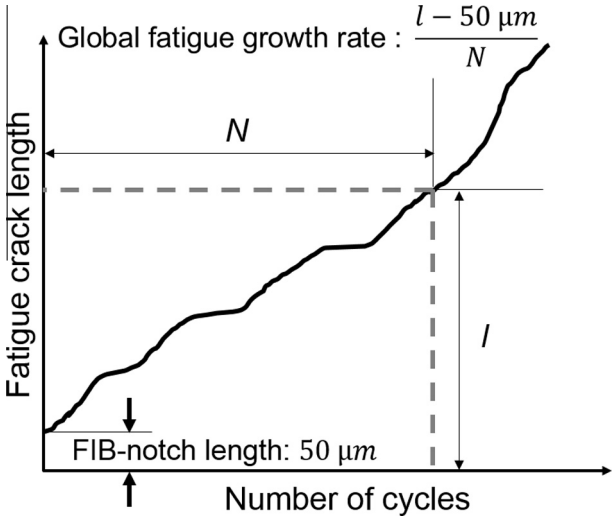

Fig. 5. Definition of global fatigue growth rate.

$$y = ax + (Y - aX) \tag{3}$$

$$y = cx + (Y - cX) \tag{4}$$

where a and c are the slopes of the approximate lines, and x and y are the fatigue crack length and the standard deviation of the logarithmic global crack growth rate, respectively.

$$\frac{d}{da}\int_{x_0}^{X}(f-(ax+(Y-aX)))^2dx = 0 \tag{5}$$

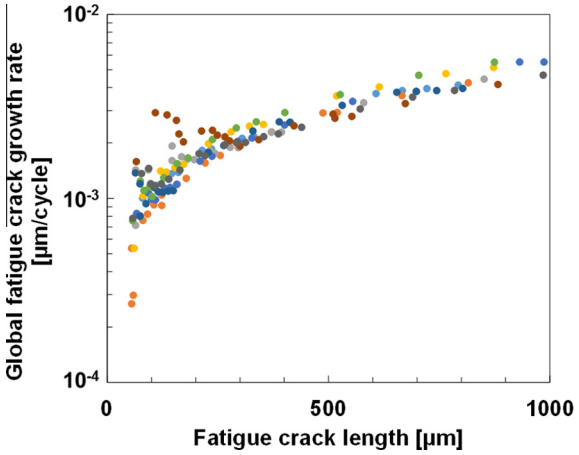

Fig. 6. Global fatigue crack growth rate of cracks longer than 1 mm in the three specimens.

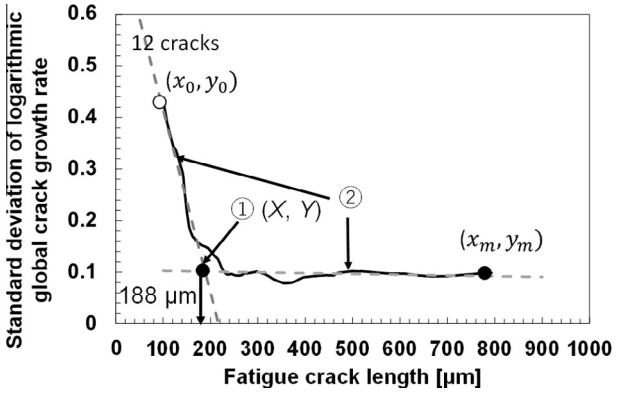

Fig. 7. Determination of l_0 by using the three specimens. Final crack length of all cracks used is longer than 1 mm.

$$\frac{d}{dc}\int_{X}^{x_m}(f-(cx+(Y-cX)))^2dx = 0 \tag{6}$$

where f is a function of the original data of the standard deviation of the logarithmic global fatigue crack growth rate plotted against the fatigue crack length.

3. Numerically find the point where J is at a minimum through repeating the first and second steps.

$$J = \int_{x_0}^{X}(f-(ax+(Y-aX)))^2dx + \int_{X}^{x_m}(f-(ax+(Y-aX)))^2dx \tag{7}$$

where J is a total amount of the squares of residual error.

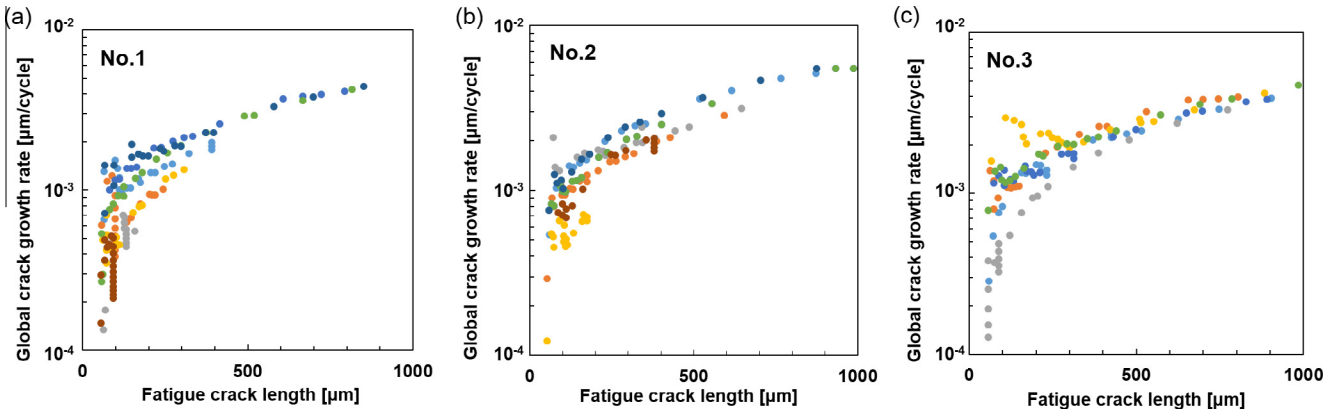

Fig. 8. Global fatigue crack growth rate obtained from (a) No. 1, (b) No. 2, and (c) No. 3. All subcracks are used in these figures.

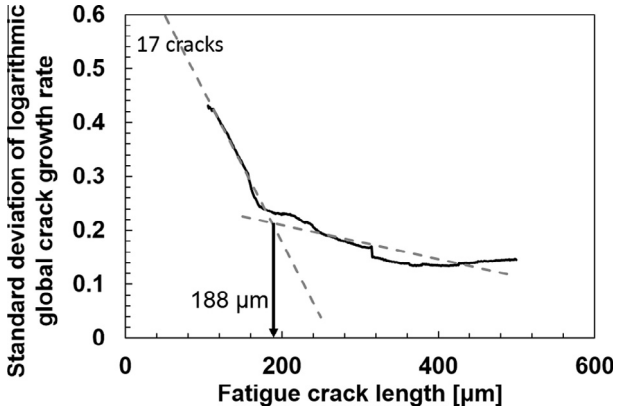

Fig. 9. Standard deviation of logarithmic crack growth rates obtained from all cracks in the three specimens.

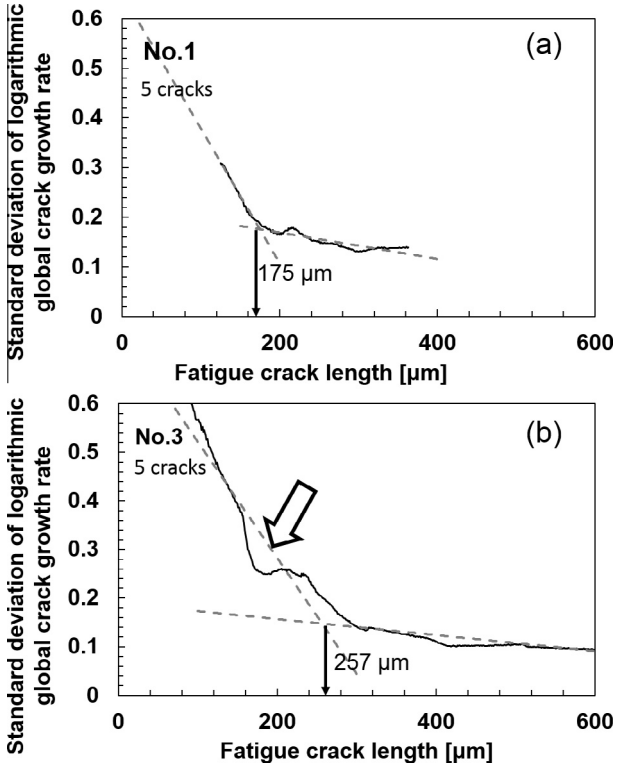

Fig. 10. Standard deviation of logarithmic global fatigue crack growth rate of specimens (a) No. 1 and (b) No. 3.

The intersection of the two lines was defined as l_0 and in this analysis was determined to be 188 μm. l_0 is approximately 7.5 times the grain size, which agrees with a previous work demonstrating that l_0 of low carbon steels is 8 times the grain size [1,22]. This determination procedure minimizes a degree of scatter due to artifacts except for the testing/measurement errors. Moreover, l_0 is generally determined by calculating the coefficient of fatigue propagation variation life in an arbitrary area and evaluating the characteristic of scatter. However, as an arbitrary area is used to determine l_0, this approach cannot be considered universal. Therefore, we proposed this determination procedure as a generalized evaluation method of l_0.

4.2. Availability of small subcracks

Toward facilitating the proposed method, we continued this study considering the data associated with small subcracks (<1 mm when the specimen broke). The consideration of subcracks can enhance statistics with a small number of specimens. Fig. 8 shows the respective growth rates of the fatigue cracks in the three specimens. These figures include small cracks that were not used in the analysis described in Section 4.1. Fig. 9 shows the statistical analysis result of the fatigue crack growth rate. Using the small subcracks, the same l_0, 188 μm, was obtained supporting the analysis of this study. In other words, the small subcracks are available.

4.3. Facilitation of l_0 determination

The small subcracks were clarified to be available in the previous section. We next attempted to determine l_0 from crack growth data in a single specimen to facilitate experiments for the determination of l_0. Fig. 10 shows two sets of standard deviation of the logarithmic global fatigue crack growth rate obtained from specimen Nos. 1 and 3. Fig. 10a shows that the data for specimen No. 1 shows a similar l_0 to that obtained from all cracks (the difference is less than 10%). In contrast, Fig. 10b shows that l_0 determined from the data in specimen No. 3 is significantly higher than the l_0 values obtained from all cracks or from specimen No. 1. The higher value in specimen No. 3 is likely due to the irregularity of the standard deviation curve around the l_0 as indicated by the arrow. A more extreme case was obtained in specimen No. 2. Fig. 11 shows the standard deviation curve of logarithmic global crack growth rate in specimen No. 2. Large scatter exists around 100–200 μm crack length in the curve as indicated by the dashed circle. When such large scatter in standard deviation is present in the curve, approximation lines cannot be drawn. Thus, determination of l_0 is impossible from the data in specimen No. 2. These facts indicate that

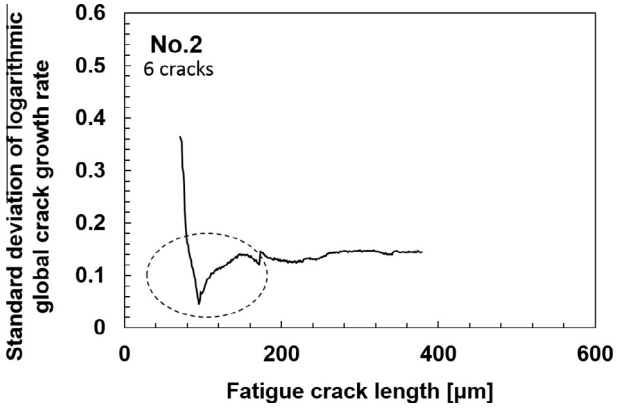

Fig. 11. Standard deviation of logarithmic global fatigue crack growth rate of specimen No. 2.

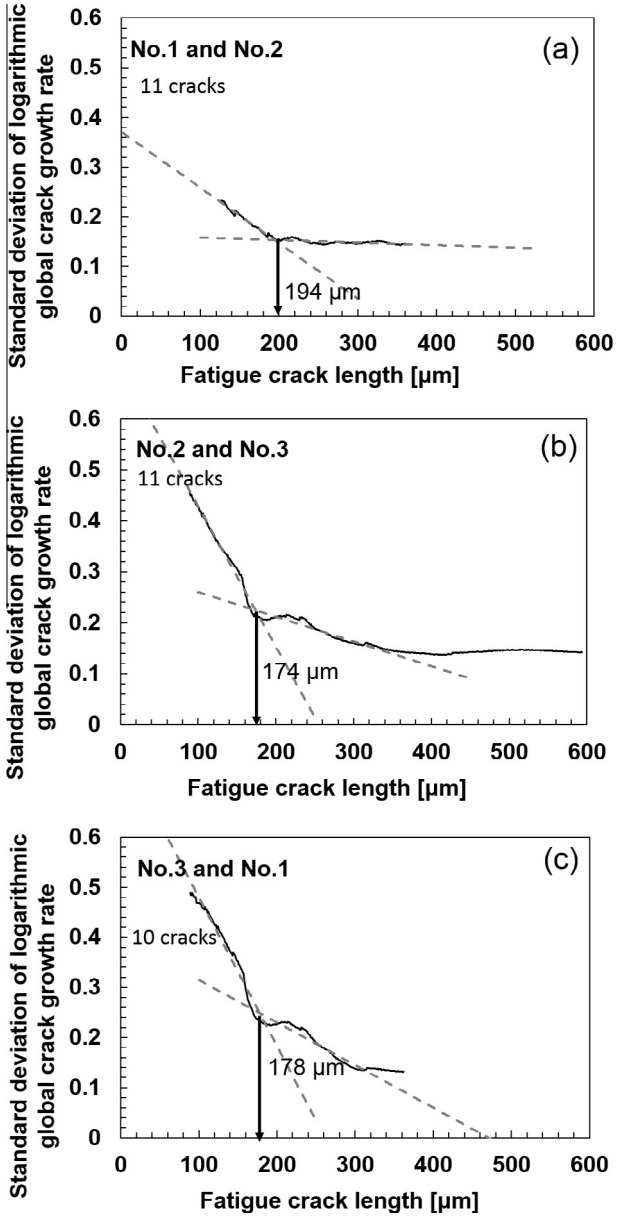

Fig. 12. Standard deviation of logarithmic crack growth rate obtained from two of the three specimens. (a) No. 1 + 2, (b) No. 2 + 3, and (c) No. 3 + 1.

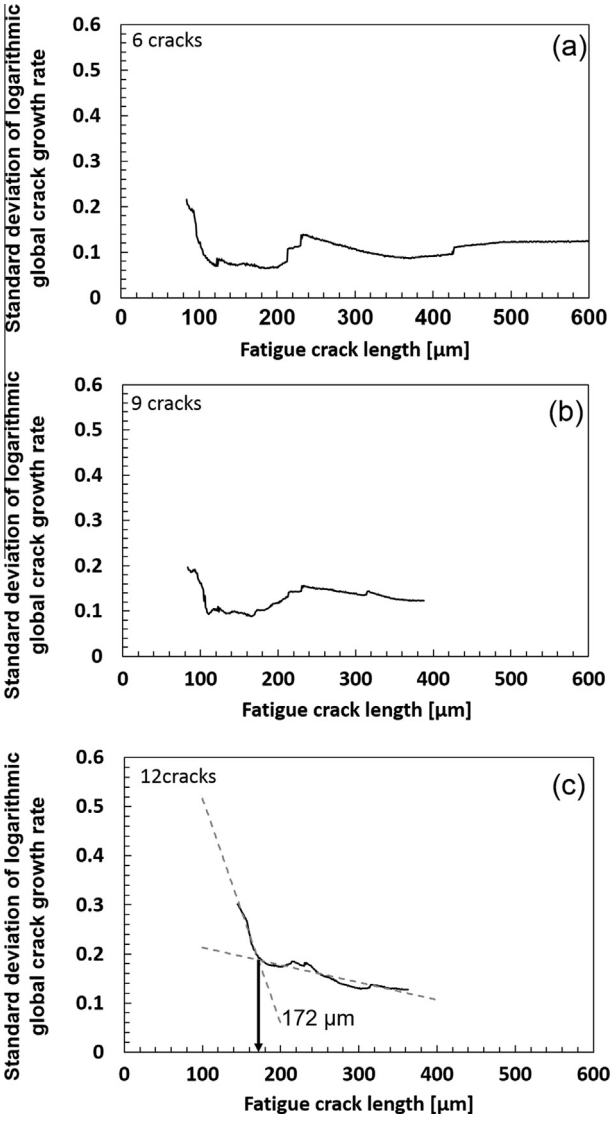

Fig. 13. Standard deviation of logarithmic crack growth rate obtained from (a) two cracks from each specimen, (b) three cracks from each specimen, and (c) four cracks from each specimen. These cracks were chosen in descending order of crack length.

determination of l_0 by using only one specimen with a similar geometry and number of FIB notches could lead to mistaken conclusions on the true nature of a microstructurally small fatigue crack growth behavior.

Although using only one specimen is not appropriate to determine l_0, our methodology still has a potential to decrease the number of test specimens required. Next, we analyzed the standard deviation of the logarithmic global fatigue crack growth rate obtained from two of the three specimens. Fig. 12 shows results of the analyses on the relationship between the standard deviation of the logarithmic global fatigue crack growth rate and the fatigue crack length. Unlike the analysis of a single specimen, all of the combinations were available for the l_0 determination. Moreover, the three l_0 obtained from the three combinations showed similar values within a 10% error. Namely, when more than 10 cracks obtained from a few specimens with the same geometry are used, l_0 can be determined reproducibly.

To confirm the reproducibility of l_0 in terms of number of cracks, other sets of combinations of cracks were analyzed as shown in Fig. 13. The cracks in Fig. 13 were chosen in descending order of crack length. When two or three cracks were used from

each specimens (the total numbers of cracks are 6 and 9, respectively), the l_0 could not be determined like the case of Fig. 11. When four cracks were used from each specimen (the total number of cracks is 12), the determined l_0 was 172 μm which is similar to the l_0 determined in Figs. 7, 9 and 12. Hence, these results also indicate that the reproducible l_0 determination by the proposed method requires more than 10 cracks. As a consequence, as long as more than 10 cracks from artificial defects are obtained, the number of specimens to determine l_0 can be decreased.

Note that some cracks in the specimen geometry did not propagate longer than 1 mm even at the maximum number of cycles as shown in Fig. 2. As the maximum number of cycles is determined by the fatigue life of a notched specimen, it is speculated that large l_0 of other materials cannot be determined by the proposed methodology even if the same specimen geometry and number of specimens are used. For instance, a large grain size is considered to provide large l_0. If the l_0 is larger than 1 mm, a diameter of a specimen must be larger than that of the specimen used in the present study. Accordingly, the position and geometry of FIB notches would also have to be modified. In addition, stress amplitude dependence of scatter in fatigue life must be noted [22,23]. The scatter has been known to increase with decreasing stress amplitude, which is attributed to sensitivity of fatigue crack initiation [1,24] and small fatigue crack growth [1,22] against microstructure. An increase in a degree of scatter with decreasing stress amplitude has negative and positive effects on applicability of the l_0 determination method. Final crack length of all cracks used in the proposed method must be longer than expected l_0. It is considered that number of cracks that do not reach the expected l_0 increases with increasing a degree of scatter in fatigue crack growth rate. Accordingly, number of specimens or artificial notches required for determining l_0 increases with decreasing stress amplitude, which is the negative effect. In contrast, the large scatter in small fatigue crack growth would provide a clearer deflection in a curve of standard deviation of logarithmic global fatigue crack growth rate, which enables more accurate determination of l_0.

5. Conclusion

In the present study, we proposed a generalized methodology to determine the transition fatigue crack length from microstructurally small to large crack growth, l_0, in order to establish a prediction model of fatigue life. This methodology minimizes artificial error, except for specimen preparations. Moreover, to minimize the number of specimens required to determine l_0, multiple micro FIB notches were introduced into a single specimen. The determined l_0 was then validated through comparisons of various l_0 values obtained by various conditions. The findings are as follows:

1. To stably determine l_0, we proposed the use of the global fatigue crack growth rate. Standard deviation of the global fatigue crack growth rate plotted against the crack length showed a distinct change in slope, which indicates l_0. The determined l_0 has a good agreement with previous studies.
2. When small subcracks were used for the analysis, the l_0 value did not change significantly. Therefore, small subcracks can be used for determination of l_0.
3. Data in a single specimen is not sufficient to obtain reproducible l_0. With the same specimen geometry, at least two specimens are required to determine l_0 of general steels. When two specimens were used, the obtained l_0 showed similar values within 10% error.

Acknowledgements

This study was supported by Cross-ministerial Strategic Innovation Promotion Program (Structural Materials for Innovation).

References

[1] Goto M. Scatter characteristics of fatigue life and the behavior of small cracks. Fatigue Fract Eng Mater Struct 1992;15:953–63.
[2] Bache MR, Evans WJ, Randle V, Wilson RJ. Characterization of mechanical anisotropy in titanium alloys. Mater Sci Eng, A 1998;257:139–44.
[3] Ritchie RO, Lankford J. Small fatigue cracks: a statement of the problem and potential solutions. Mater Sci Eng 1986;84:11–6.
[4] Miller KJ. The short crack problem. Fatigue Fract Eng Mater Struct 1982;5:223–32.
[5] Hussain K. Short fatigue crack behaviour and analytical models: a review. Eng Fract Mech 1997;58:327–54.
[6] Lankford J. Initiation and early growth of fatigue cracks in high strength steel. Eng Fract Mech 1977;9:617–24.
[7] Navarro A, de los Rios ER. A microstructurally-short fatigue crack growth equation. Fatigue Fract Eng Mater Struct 1988;11:383–96.
[8] Tokaji K, Ogawa T, Harada Y. The growth of small fatigue cracks in a low carbon steel; the effect of microstructure and limitation of linear elastic fracture mechanics. Fatigue Fract Eng Mater Struct 1986;9:205–17.
[9] Rodopoulos CA, de los Rios ER. Theoretical analysis on the behaviour of short fatigue cracks. Int J Fatigue 2002;24:719–24.
[10] McDowell DL. An engineering model for propagation of small cracks in fatigue. Eng Fract Mech 1997;56:357–77.
[11] Sakamoto J, Takahashi Y, Aono Y, Noguchi H. Method for assessing applicability of an artificial flaw as a small initial crack for fatigue limit evaluation and its application to a drill hole and an FIB processed sharp notch in annealed 0.45% carbon steel; 2013.
[12] Hironobu N, Masahiro G, Norio K. A small-crack growth law and its related phenomena. Eng Fract Mech 1992;41:499–513.
[13] Fukumura N, Suzuki T, Hamada S, Tsuzaki K, Noguchi H. Mechanical examination of crack length dependency and material dependency on threshold stress intensity factor range with Dugdale model. Eng Fract Mech 2015;135:168–86.
[14] Sugeta A, Uematsu Y, Hashimoto A, Jono M. Atomic force microscopy of fatigue crack growth behavior in the low K region. Int J Fatigue 2004;26:1159–68.
[15] Düber O, Künkler B, Krupp U, Christ HJ, Fritzen CP. Experimental characterization and two-dimensional simulation of short-crack propagation in an austenitic–ferritic duplex steel. Int J Fatigue 2006;28:983–92.
[16] Laird C, de la Veaux R. Additional evidence for the plastic blunting process of fatigue crack propagation. Metall Trans A 1977;8:657–64.
[17] Richards CE, Lindley TC. The influence of stress intensity and microstructure on fatigue crack propagation in ferritic materials. Eng Fract Mech 1972;4:951–78.
[18] Bennett VP, McDowell DL. Crack tip displacements of microstructurally small surface cracks in single phase ductile polycrystals. Eng Fract Mech 2003;70:185–207.
[19] Xi Z-J, Koyama M, Yoshida Y, Yoshimura N, Ushioda K, Noguchi H. Effects of cementite morphology on short-fatigue-crack propagation in binary Fe–C steel. Philos Mag Lett 2015;95:384–91.
[20] Simonovski I, Nilsson K-F, Cizelj L. The influence of crystallographic orientation on crack tip displacements of microstructurally small, kinked crack crossing the grain boundary. Comput Mater Sci 2007;39:817–28.
[21] Chakravarthula SS, Qiao Y. Fatigue crack growth in a coarse-grained iron–silicon alloy. Int J Fatigue 2005;27:1210–4.
[22] Goto M. Statistical investigation of the behaviour of small cracks and fatigue life in carbon steels with different ferrite grain sizes. Fatigue Fract Eng Mater Struct 1994;17:635–49.
[23] Schijve J. Statistical distribution functions and fatigue of structures. Int J Fatigue 2005;27:1031–9.
[24] Przybyla C, Prasannavenkatesan R, Salajegheh N, McDowell DL. Microstructure-sensitive modeling of high cycle fatigue. Int J Fatigue 2010;32:512–25.